RSC Advances

PAPER

View Article Online
View Journal | View Issue

Cite this: *RSC Adv.*, 2018, **8**, 26998

Conversion of dilute nitrous oxide (N_2O) in N_2 and N_2–O_2 mixtures by plasma and plasma-catalytic processes†

Xing Fan, *[a] Sijing Kang,[a] Jian Li[a] and Tianle Zhu[b]

A coaxial dielectric barrier discharge (DBD) reactor has been developed for plasma and plasma-catalytic conversion of dilute N_2O in N_2 and N_2–O_2 mixtures at both room and high temperature (300 °C). The effects of catalyst introduction, O_2 content and inlet N_2O concentration on N_2O conversion and the mechanism involved in the conversion of N_2O have been investigated. The results show that N_2O in N_2 could be effectively decomposed to N_2 and O_2 by plasma and plasma-catalytic processes at both room and high temperature, with much higher decomposition efficiency at 300 °C than at room temperature for the same discharge power. Under an N_2–O_2 atmosphere, however, N_2O could be removed only at high temperature, producing not only N_2 and O_2 but also NO and NO_2. Production and conversion of N_2O occur simultaneously during the plasma and plasma-catalytic processing of N_2O in a N_2–O_2 mixture, with production and conversion being the dominant processes at room and high temperature, respectively. N_2O conversion increases with the increase of discharge power and decreases with the increase of O_2 content. Increasing the inlet N_2O concentration from 100 to 400 ppm decreases the conversion of N_2O under an N_2 atmosphere but increases that under an N_2–O_2 atmosphere. Concentrating N_2O in the N_2–O_2 mixture could alleviate the negative influence of O_2 by increasing the involvement of plasma reactive species (*e.g.*, $N_2(A^3\Sigma_u^+)$ and $O(^1D)$) in N_2O conversion. Packing the discharge zone with a RuO_2/Al_2O_3 catalyst significantly enhances the conversion of N_2O and improves the selectivity of N_2O decomposition under an N_2–O_2 atmosphere, revealing the synergy of plasma and catalyst in promoting N_2O conversion, especially its decomposition to N_2 and O_2.

Received 1st July 2018
Accepted 21st July 2018

DOI: 10.1039/c8ra05607b

rsc.li/rsc-advances

1. Introduction

Nitrous oxide (N_2O) emitted from various human activities including agriculture (soil cultivation and the use of nitrogen-fertilizers), biomass burning, fossil fuel combustion, industrial processes (production of adipic and nitric acids), and wastewater treatment is the third most significant anthropogenic greenhouse gas and the largest stratospheric-ozone-depleting substance.[1–3] Limiting the formation of N_2O is the best solution to reduce N_2O emissions from the agricultural sector and uncontrolled biomass burning taking into account the diffuse character of these emissions, while employment of after-treatment technologies is important for control of N_2O emissions from combustion and industrial sources.[3]

Technologies developed and adopted so far for abatement of N_2O are mainly based on catalysis, including non-selective catalytic reduction (NSCR), selective catalytic reduction (SCR), and direct catalytic decomposition.[1,3–8] Among these technologies, the direct catalytic decomposition of N_2O to N_2 and O_2 has received great attention due to simplicity and high efficiency and significant research efforts have been focused on development of novel catalytic materials with satisfactory activity at relatively low temperatures.[1,3,5–8] As a promising alternative to develop new catalysts, combination of catalysts with non-thermal plasma has been widely investigated in recent years for treatment of a variety of air contaminants such as volatile organic compounds (VOCs) and nitrogen oxides (NO_x).[9–16] The synergetic effects between plasma and catalysis include initiating chemical reactions at low temperature and improving products selectivity.[9–16] In fact, plasma and plasma-catalysis systems have also been investigated for decomposition of N_2O, with nitrogen or argon as the background gas in most cases.[17–22] These oxygen-free systems proved to be effective in decomposing N_2O even at room temperature.[17–22] In real exhaust gases, however, O_2 always coexists with N_2O and N_2 and it is therefore of great significance to investigate the N_2O conversion behavior under N_2–O_2 atmosphere.[3]

In a recent study by Jo *et al.*,[23] O_2 in N_2–O_2–N_2O mixture was verified to have obviously adverse effects on the plasma-catalytic

[a]*Key Laboratory of Beijing on Regional Air Pollution Control, College of Environmental and Energy Engineering, Beijing University of Technology, Beijing 100124, China. E-mail: fanxing@bjut.edu.cn*

[b]*School of Space and Environment, Beihang University, Beijing 100191, China*

† Electronic supplementary information (ESI) available. See DOI: 10.1039/c8ra05607b

decomposition of N_2O. Besides the negative influence of O_2 on the catalytic decomposition of N_2O, the intrinsic formation of N_2O by discharge in N_2–O_2 should have also contributed to the decreasing N_2O conversion with increasing O_2 content, which however was not taken into account in that study.[23] From our perspective, a better understanding of both N_2O production and conversion processes in the presence of O_2 is essential for optimizing the plasma-catalytic decomposition of N_2O. On the other hand, Jo *et al.*[23] inferred from the thermodynamic calculations that N_2O was mainly decomposed into N_2 and O_2 in the presence of O_2. However, Krawczyk *et al.*[24,25] found that N_2O in mixtures with O_2 or air was both oxidized to NO and decomposed to N_2 and O_2 by gliding arc discharge, combined with or without a catalytic bed. Oxidation of N_2O into NO and reusing NO for production of nitric acid is a profitable method for reducing concentrated N_2O emissions, *e.g.*, in adipic acid plants.[24] For removal of dilute N_2O from sources such as nitric acid production and fluidized bed combustion, however, decomposition of N_2O into N_2 and O_2 would be more desired.[3]

The aim of this study is to investigate the conversion behavior and mechanism of dilute N_2O in plasma and plasma-catalytic processes, in both the presence and absence of O_2 and at both room and high temperature (300 °C). For this purpose, a coaxial dielectric barrier discharge (DBD) reactor was constructed, to generate plasma and to combine plasma with catalysts. RuO_2/Al_2O_3 was chosen as the catalyst besides Al_2O_3 for plasma-catalytic conversion of N_2O due to its reported good performance for catalytic N_2O decomposition.[26] The effects of catalyst (Al_2O_3 or RuO_2/Al_2O_3) introduction, O_2 content (0–20%, volumetric) and inlet N_2O concentration (100–400 ppm, volumetric) on the conversion of N_2O were systematically examined. In order to elucidate the mechanism of N_2O conversion, the production of N_2O by discharge in N_2–O_2 mixture with and without catalyst was also investigated and products/byproducts generated in these processes were analyzed in detail.

2. Experimental

2.1 Experimental set-up

A schematic diagram of the experimental system is shown in Fig. 1. It consists of reaction gas supply, a DBD reactor with an alternating current (AC) high voltage power supply (0–100 kV, 50–500 Hz, sinusoidal wave), and analytical instrumentation. The reaction gas which was fed into the reactor at a total flow rate of 1 L min^{-1} at ambient temperature and pressure (around 20 °C, 100 kPa) throughout this work was prepared by mixing pure N_2, O_2, and N_2O in N_2 (Beijing HaiRui Tongda Gas Technology Co., Ltd., China) whose flow rates were controlled by a set of mass flow controllers (MFC, D07-7, Beijing Sevenstar Electronics Co., Ltd., China). O_2 content in the feed gas was adjusted to 0%, 5%, 10% or 20% while inlet concentration of N_2O ranged from 0 to 400 ppm.

A quartz glass tube reactor (length: 600 mm; inner diameter: 29 mm; thickness: 1.5 mm) was used with a concentric tungsten wire (diameter: 1.4 mm) acting as the discharge electrode and an aluminum foil (50 mm in length) wrapping around the glass tube as the ground electrode. For the plasma-catalytic process, Al_2O_3 or RuO_2/Al_2O_3 catalyst pellets (20 g, 3–5 mm in diameter) were packed in the space between the discharge electrode and the tube at near maximum packing density, with an apparent volume of *ca.* 27 mL. The plasma/plasma-catalytic reactor was installed in normal indoor environments or in a temperature-controlled tube furnace to obtain room temperature and high temperature (300 °C) reaction conditions, respectively.

2.2 Experimental methods

2.2.1 Preparation and characterization of catalyst. Commercial γ-Al_2O_3 pellets (Brunauer–Emmett–Teller (BET) specific surface area 226 m^2 g^{-1}, specific pore capacity 0.48 mL g^{-1}, Tianjin Fuchen Chemical Reagents Factory, China) were used as the catalyst as well as the support of RuO_2/Al_2O_3 catalyst. For the preparation of RuO_2/Al_2O_3, a given amount of γ-Al_2O_3 pellets were impregnated with an aqueous solution of $RuCl_3$ (99% purity, J&K Scientific). After the impregnation, drying overnight at 110 °C and calcining at 550 °C for 6 h in air atmosphere were performed. The nominal loading amount of Ru over Al_2O_3 was 2.4 wt% and the BET specific surface area of the prepared RuO_2/Al_2O_3 catalyst was 194 m^2 g^{-1}, measured by N_2 adsorption at −196 °C on a surface area and pore size analyzer (Micromeritics Gemini V, USA).

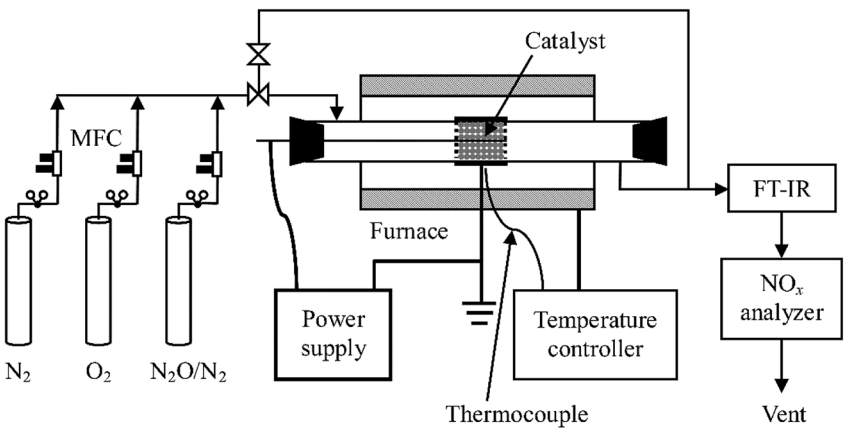

Fig. 1 Schematic diagram of the experimental set-up.

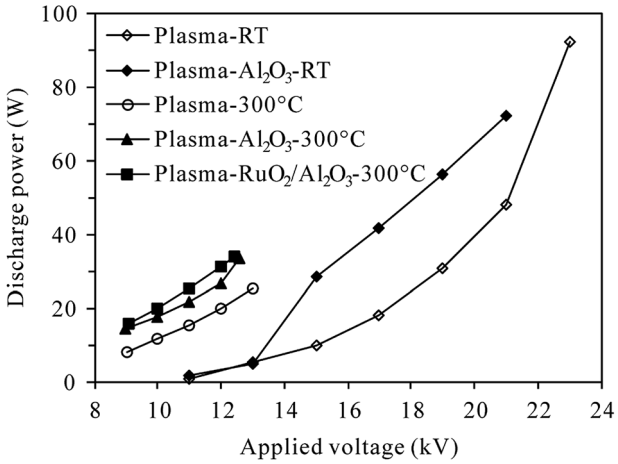

Fig. 2 Dependence of discharge power on the applied voltage at room temperature (RT) and 300 °C (inlet N_2O: 0 ppm; O_2 content: 5%).

In addition, X-ray diffraction (XRD) patterns of Al_2O_3 and RuO_2/Al_2O_3 catalysts before and after use in plasma-catalytic conversion of N_2O were obtained using a Bruker D8 Discover diffractometer (Co Kα radiation, 35 kV, 30 mA).

2.2.2 Measurement of discharge characteristics. The DBD reactor was energized at 200 Hz in the range of 9–23 kV (root-mean-square (RMS) value) in this study. The applied voltage and discharge current was measured using a 1000:1 high voltage probe (P6015A, Tektronix, USA) and a current monitor (UT61D, UNI-T, China), respectively. The discharge power delivered to the reactor was calculated by multiplying the time-dependent voltage and current. Fig. 2 presents typical discharge power values of plasma and plasma-catalytic reactors at room temperature and 300 °C as functions of applied voltage. It is worth pointing out that although higher discharge power could be delivered to the reactors under higher reaction temperature (300 °C) for a given applied voltage, the breakdown voltage and maximum applicable discharge power were much lower at 300 °C than those at room temperature.

2.2.3 Analysis of gas components and calculation of N_2O conversion. The reactor outlet gas stream was analyzed using an on-line Fourier transform infrared (FT-IR) spectrometer (Nicolet iS10, Thermo-Scientific, USA) equipped with a heated gas cell (optical path length: 2.4 m; volume: 300 mL; temperature: 100 °C) and a deuterated triglicine sulfate (DTGS) KBr detector. Spectra were recorded automatically every 35 s (average of 16 scans from 4000 to 650 cm^{-1} with a resolution of 4 cm^{-1}) from the start to the end of each experiment, with the background spectra being recorded under dry N_2 before the experiment. For quantification of N_2O, NO and NO_2, the FT-IR spectrometer was calibrated using standard gases of these components, with measurement uncertainty of ±1 ppm. Besides, NO and NO_2 concentrations were also measured by a NO_x analyzer (42i-HL, Thermo-Scientific, USA, uncertainty ±1%). Considering the relative low infrared absorption of NO and potential interference by H_2O, concentration of NO was mainly determined by the NO_x analyzer in this work while that of NO_2 by the FT-IR spectrometer.

The conversion of N_2O is calculated based on its inlet ($C_{N_2O,in}$, ppm) and outlet concentrations ($C_{N_2O,out}$, ppm), as shown in eqn (1).

$$\text{Conversion of } N_2O = \frac{C_{N_2O,in} - C_{N_2O,out}}{C_{N_2O,in}} \times 100\% \quad (1)$$

The selectivity of NO, NO_2 and NO_x (NO + NO_2) produced from N_2O conversion is calculated based on the N-balance as follows:

$$\text{Selectivity of NO} = \frac{C_{NO,\text{with } N_2O} - C_{NO,\text{w/o } N_2O}}{2 \times (C_{N_2O,in} - C_{N_2O,out})} \times 100\% \quad (2)$$

$$\text{Selectivity of } NO_2 = \frac{C_{NO_2,\text{with } N_2O} - C_{NO_2,\text{w/o } N_2O}}{2 \times (C_{N_2O,in} - C_{N_2O,out})} \times 100\% \quad (3)$$

$$\text{Selectivity of } NO_x = \text{selectivity of NO} + \text{selectivity of } NO_2 \quad (4)$$

where $C_{NO,\text{with } N_2O}$, $C_{NO,\text{w/o } N_2O}$ and $C_{NO_2,\text{with } N_2O}$, $C_{NO_2,\text{w/o } N_2O}$ indicate the outlet concentrations of NO and NO_2 (ppm) detected with and without N_2O in the inlet gas, respectively; 2 is the number ratio of nitrogen atoms of N_2O and NO/NO_2.

3. Results and discussion

3.1 Conversion of N_2O at room temperature

3.1.1 Conversion of N_2O under N_2 atmosphere. Fig. 3 shows the conversion of 100 ppm-N_2O in N_2 as functions of discharge power in plasma and plasma-Al_2O_3 reactors at room temperature. It can be seen that without O_2 in the reaction gas, N_2O can be effectively decomposed by both plasma and plasma-Al_2O_3 processes. The N_2O conversion increased with the increase of discharge power, which can be easily ascribed to the

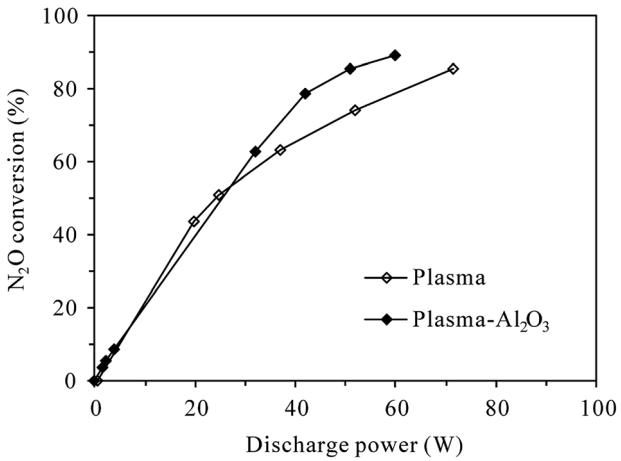

Fig. 3 Dependence of N_2O conversion on the discharge power in plasma and plasma-Al_2O_3 reactors at room temperature (inlet N_2O: 100 ppm; O_2 content: 0%).

increment of active species for N_2O decomposition at higher discharge power. In an intensive study of N_2O conversion by pulsed corona discharge in N_2, Zhao *et al.*[18] confirmed that among the active species, the first excited state of molecular nitrogen, *i.e.*, $N_2(A^3\Sigma_u^+)$ produced by electron impact excitation of nitrogen molecules (reaction (R1)[27]), appeared to be mainly involved in the decomposition of N_2O through reaction (R2). Reaction (R2) was also concluded to be responsible for the conversion of N_2O in N_2 DBD plasma by Trinh *et al.*[20] With the increase of discharge power, more $N_2(A^3\Sigma_u^+)$ would be produced for N_2O decomposition due to the increase of energetic electrons. As shown in Fig. 3, the highest N_2O conversion was 85.7% and 89.4% observed at the highest discharge power of 71.6 W and 59.8 W tested for plasma and plasma-Al_2O_3 process, respectively. Packing with Al_2O_3 catalyst slightly facilitated the decomposition of N_2O in N_2, probably by enhancing the electric fields around the contact points of dielectric Al_2O_3 pellets.[19]

$$N_2 + e \rightarrow N_2(A^3\Sigma_u^+) + e \quad (R1)$$

$$N_2(A^3\Sigma_u^+) + N_2O \rightarrow 2N_2 + O \quad (R2)$$

3.1.2 Conversion and production of N_2O under N_2–O_2 atmosphere. Once O_2 (5%, 10% or 20%) was added into the reaction gas, N_2O could not be decomposed anymore at room temperature, no matter in the presence or absence of Al_2O_3 catalyst. In fact, N_2O concentration increased due to additional production of N_2O, which was widely accepted to proceed mainly by the reaction of $N_2(A^3\Sigma_u^+)$ with oxygen, as shown in (R3).[27–29] Obviously, $N_2(A^3\Sigma_u^+)$ plays an important role in both production and decomposition of N_2O *via* (R3) and (R2), respectively.

$$N_2(A^3\Sigma_u^+) + O_2 \rightarrow N_2O + O \quad (R3)$$

Fig. 4 compares the increased concentration of N_2O ($C_{N_2O,out} - C_{N_2O,in}$) under different O_2 contents with and without 100 ppm-N_2O in the N_2–O_2 mixture. As can be seen from Fig. 4(a), no matter with or without N_2O in the inlet gas, the increased concentration of N_2O in the plasma reactor first increased and then decreased with the increase of discharge power, attaining a maximum at *ca.* 35 W. The reason for this may be that the increase of discharge power promotes not only the formation of N_2O *via* (R3), but also N_2O loss by (R2) and/or (R4)–(R6).[27,29–31] Higher discharge power means that more energy could be used to excite/dissociate N_2 and O_2 molecules, producing more reactive species such as $N_2(A^3\Sigma_u^+)$ and $O(^1D)$. At relatively low discharge power, the concentration of N_2O increased with increasing discharge power due to the enhanced production of $N_2(A^3\Sigma_u^+)$ species for N_2O formation (R3). With the increase of N_2O concentration and increasing production of reactive species ($N_2(A^3\Sigma_u^+)$ and $O(^1D)$), the probability of N_2O loss reactions ((R2), (R5) and (R6)) raised, explaining the observed decrease of N_2O concentration at higher discharge power. In the whole discharge power range tested, however, the production of N_2O surpassed the loss since the increased concentration of N_2O was always positive.

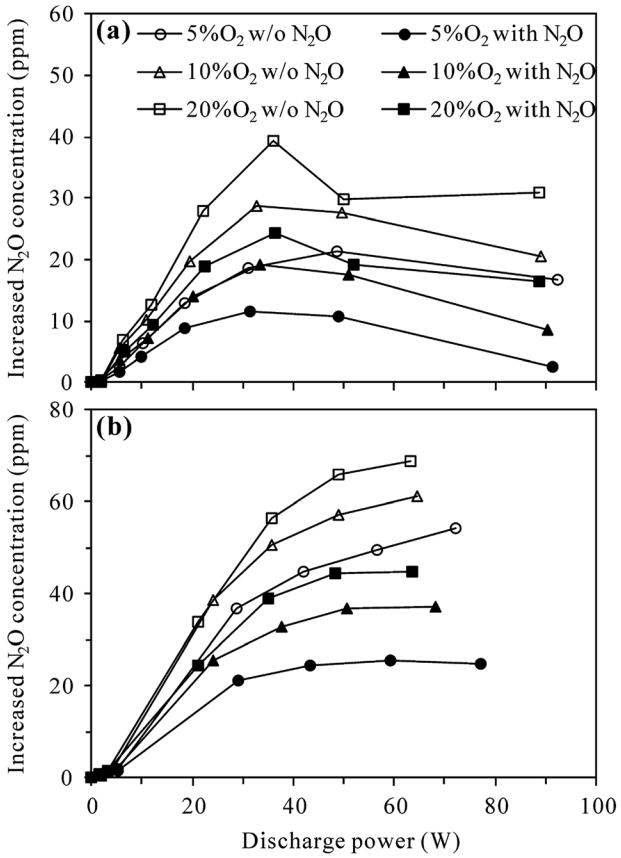

Fig. 4 Effects of N_2O presence in N_2–O_2 mixture on the production of N_2O by discharge in (a) plasma and (b) plasma-Al_2O_3 reactors at room temperature (inlet N_2O: 0 or 100 ppm; O_2 content: 5%, 10% or 20%).

$$O_2 + e \rightarrow O(^3P) + O(^1D) + e \quad (R4)$$

$$O(^1D) + N_2O \rightarrow NO + NO \quad (R5)$$

$$O(^1D) + N_2O \rightarrow N_2 + O_2 \quad (R6)$$

Fig. 4(a) also shows that in both the presence and absence of N_2O in the inlet gas, more N_2O was produced in the plasma reactor under higher O_2 contents for a given discharge power, indicating the important role of O_2 in N_2O production.[27,29] Compared with the case without N_2O in the inlet gas, introduction of 100 ppm-N_2O significantly reduced the production of N_2O under all O_2 contents. In the presence of initial N_2O, more $N_2(A^3\Sigma_u^+)$ species would be consumed in N_2O decomposition (reaction (R2)), reducing the amount of $N_2(A^3\Sigma_u^+)$ species for N_2O production (reaction (R3)) as a result.

Compared to plasma alone, more N_2O was produced in the plasma-Al_2O_3 reactor (Fig. 4(b)) under otherwise similar conditions, indicating the promotion effects of Al_2O_3 catalyst on N_2O formation by discharge. In a study focusing on N_2O formation by DBD in N_2–O_2 mixtures, Tang *et al.* also reported similar increase of N_2O production by packing Al_2O_3 in the discharge zone and surface oxygen species (Al_2O_3–O*) brought by Al_2O_3

into the plasma chemical process (reaction (R7)) was considered as the main reason.[29]

$$N_2(A^3\Sigma_u^+) + Al_2O_3\text{–}O^* \rightarrow N_2O + Al_2O_3 \quad (R7)$$

where * represents an active site on the catalyst and O* represents atomic oxygen bound to the site.[29]

In the presence of Al_2O_3 catalyst (Fig. 4(b)), the increased concentration of N_2O first increased and then tended to reach equilibrium values with the increase of discharge power, demonstrating that N_2O production was counterbalanced by N_2O loss at high discharge power, especially when N_2O was introduced into the inlet gas. As in the plasma case, introduction of 100 ppm-N_2O into the N_2–O_2 mixture also resulted in less production of N_2O in the plasma-Al_2O_3 reactor (Fig. 4(b)).

In addition, it is worth mentioning that although the presence of 100 ppm-N_2O in the N_2–O_2 mixture significantly affected the production of N_2O by discharge, it did not induce significant changes to the formation behavior of NO and NO_2 in both plasma (Fig. S1†) and plasma-Al_2O_3 reactors (Fig. S2†) at room temperature.

3.2 Conversion of N_2O at high temperature

In order to decompose N_2O in the O_2-containing atmosphere, the reaction temperature was raised to 300 °C in this section and RuO_2/Al_2O_3 was also investigated besides Al_2O_3 for plasma-catalytic decomposition of N_2O.

3.2.1 Effects of catalyst introduction. Fig. 5 presents the conversion of N_2O in plasma and plasma-catalytic reactors as functions of discharge power at 300 °C. The concentrations of N_2O and O_2 in the inlet gas were 400 ppm and 5%, respectively. In the absence of plasma (at discharge power of 0 W), a small conversion of N_2O (1.8%) was observed in the plasma-RuO_2/Al_2O_3 reactor while no N_2O was converted in the plasma or plasma-Al_2O_3 reactors. This indicated that N_2O was stable in the gas phase and over the Al_2O_3 catalyst at as high as 300 °C, but RuO_2/Al_2O_3 catalyst did show low activity for N_2O decomposition. The conversion of N_2O increased with the increase of discharge power no matter the catalyst was introduced or not, demonstrating that N_2O in N_2–O_2 mixture could indeed be removed by plasma and plasma-catalytic processes at high temperature. When no catalyst was packed in the discharge zone, however, the N_2O conversion was very low, reaching only 3.8% at the highest discharge power tested (21.8 W). Introducing catalyst, especially RuO_2/Al_2O_3 into the discharge zone greatly improved the conversion of N_2O. Considering that Al_2O_3 and RuO_2/Al_2O_3 catalysts alone showed no or very low activity for N_2O decomposition at 300 °C, the enhanced conversion of N_2O in the plasma-catalytic process could only be attributed to the synergy of plasma and catalyst in N_2O conversion.[23,24] The highest conversion of N_2O, however, was only 31.2% observed in the plasma-RuO_2/Al_2O_3 reactor. As stated in Section 2.2.2, the maximum applicable discharge power was limited at 300 °C due to easy breakdown of the reactor wall material (quartz glass). Further increase of the discharge power and N_2O conversion may be achieved by using reactors with higher resistance to breakdown, such as alumina ceramic tube reactor.[23]

On the other hand, Fig. 6 shows the production of N_2O in the plasma and plasma-catalytic processes at 300 °C without N_2O in the inlet gas (inlet gas composition: 5% O_2 + N_2). It can be seen that for both plasma and plasma-catalytic processes, N_2O concentration increased almost linearly with discharge power in the range tested. Packing catalyst in the discharge zone greatly enhanced the production of N_2O, but no significant difference was observed in N_2O production between the plasma-Al_2O_3 and plasma-RuO_2/Al_2O_3 systems. Compared to the room-temperature case (Fig. 4), much less N_2O was produced at 300 °C for the same O_2 content (5%) and discharge power. Considering the low conversion of N_2O obtained, especially in the plasma and plasma-Al_2O_3 processes (Fig. 5), the observed less production of N_2O (Fig. 6) should be mainly due to the low effectiveness of N_2O formation reactions (*e.g.*, (R3)) at high temperature. In other words, high reaction temperature is

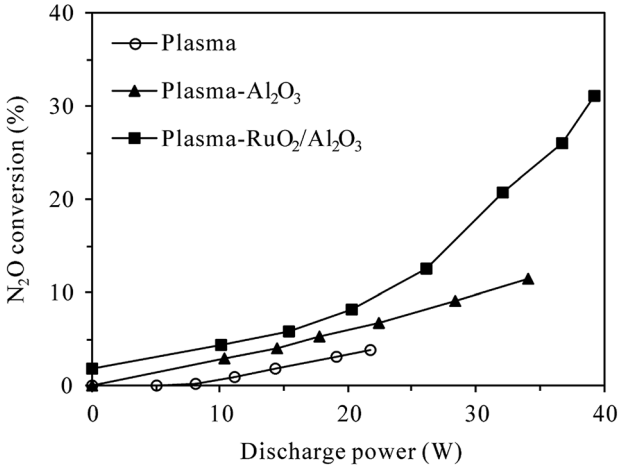

Fig. 5 Dependence of N_2O conversion on the discharge power in plasma and plasma-catalytic reactors at 300 °C (inlet N_2O: 400 ppm; O_2 content: 5%).

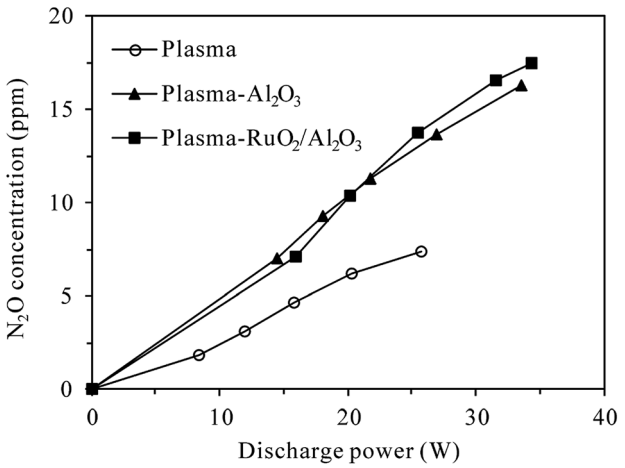

Fig. 6 Dependence of N_2O production on the discharge power in plasma and plasma-catalytic reactors at 300 °C (inlet N_2O: 0 ppm; O_2 content: 5%).

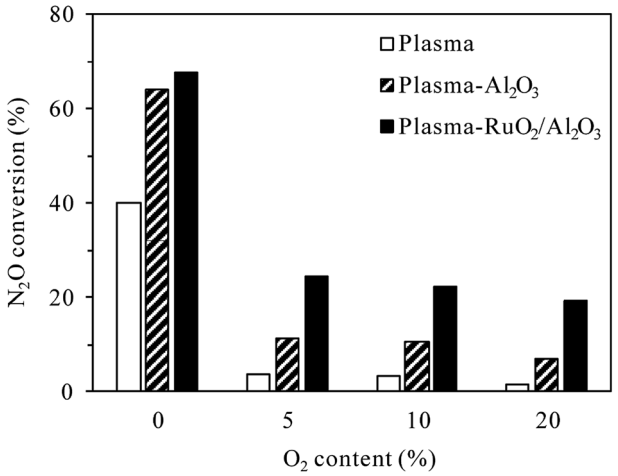

Fig. 7 Effects of O_2 content on N_2O conversion in plasma and plasma-catalytic reactors at 300 °C (inlet N_2O: 400 ppm; discharge power: 22 W for the plasma process and 34 W for the plasma-catalytic process).

favorable not only for conversion of N_2O but also for reduction of N_2O formation by discharge in N_2–O_2 mixture. At high temperature (300 °C), introducing catalyst, especially RuO_2/Al_2O_3 into the discharge zone significantly enhances the conversion of N_2O, overbalancing its promoting effects on N_2O production, which finally results in effective removal of N_2O from the N_2–O_2 mixture (Fig. 5).

3.2.2 Effects of O_2 content. O_2 content can largely influence the plasma/plasma-catalytic conversion of N_2O due to the intrinsic formation of N_2O in N_2–O_2 plasma. Fig. 7 shows the effects of O_2 content on N_2O conversion (inlet N_2O 400 ppm) in plasma and plasma-catalytic processes at 300 °C. In both the presence and absence of catalyst, the conversion of N_2O drastically decreased when the O_2 content was changed from 0 to 5%, revealing that O_2 inhibited the plasma and plasma-catalytic decomposition of N_2O significantly. Jo *et al.*[23] attributed the negative influence of O_2 on catalytic and plasma-catalytic decomposition of N_2O to the competitive adsorption of O_2 onto the active sites over RuO_2/Al_2O_3 catalyst. Besides this, O_2 could significantly decrease the electron density and the formation rate of $N_2(A^3\Sigma_u^+)$ species in plasma due to its electronegative characteristics.[32–35] In addition to directly react with $N_2(A^3\Sigma_u^+)$ species to produce additional N_2O (reaction (R3)), O_2 could also reduce the amount of $N_2(A^3\Sigma_u^+)$ species by dissociative quenching (reaction (R8)) due to its low dissociation energy (5.2 eV per molecule).[32,36] The decrease of $N_2(A^3\Sigma_u^+)$ species for N_2O decomposition, additional production of N_2O as well as the competitive adsorption of O_2 over the catalyst sites should all contribute to the dramatic decrease of N_2O conversion in the presence of O_2.

$$N_2(A^3\Sigma_u^+) + O_2 \rightarrow N_2 + O + O \quad \text{(R8)}$$

As also shown in Fig. 7, for the same discharge power of 34 W, N_2O conversion in the plasma-Al_2O_3 process decreased from 64.3% for 0% O_2 content to 11.4% for 5% O_2 content, while that in the plasma-RuO_2/Al_2O_3 process decreased from 67.9% to 24.4%. The superiority of RuO_2/Al_2O_3 over Al_2O_3 was more pronounced in the O_2-containing cases. Further increase of the O_2 content from 5% to 10% and 20% caused further decrease of the N_2O conversion, but the extent of decrease was less prominent.

3.2.3 Effects of inlet N_2O concentration. The inlet concentration of N_2O can also be an important factor influencing the plasma and plasma-catalytic decomposition processes. The effects of inlet N_2O concentration on N_2O conversion at 300 °C with 0% and 5% O_2 in the reaction gas are presented in Fig. 8. For the plasma process (Fig. 8(a)), at a given discharge power of 22 W, the conversion of N_2O without O_2 significantly decreased from 71.6% to 40.0% while that with 5% O_2 slightly increased from 1.2% to 3.8% when the inlet N_2O concentration was increased from 100 to 400 ppm. It is obvious that higher inlet concentration leads to lower conversion of N_2O in N_2 plasma due to the competitive consumption of reactive species for N_2O decomposition ($N_2(A^3\Sigma_u^+)$) by increasing N_2O molecules. In the presence of 5% O_2, however, the conversion of N_2O was enhanced by injecting more N_2O into the reaction gas. The reason for this may be that more $N_2(A^3\Sigma_u^+)$ species would be consumed in the decomposition of higher-concentration N_2O

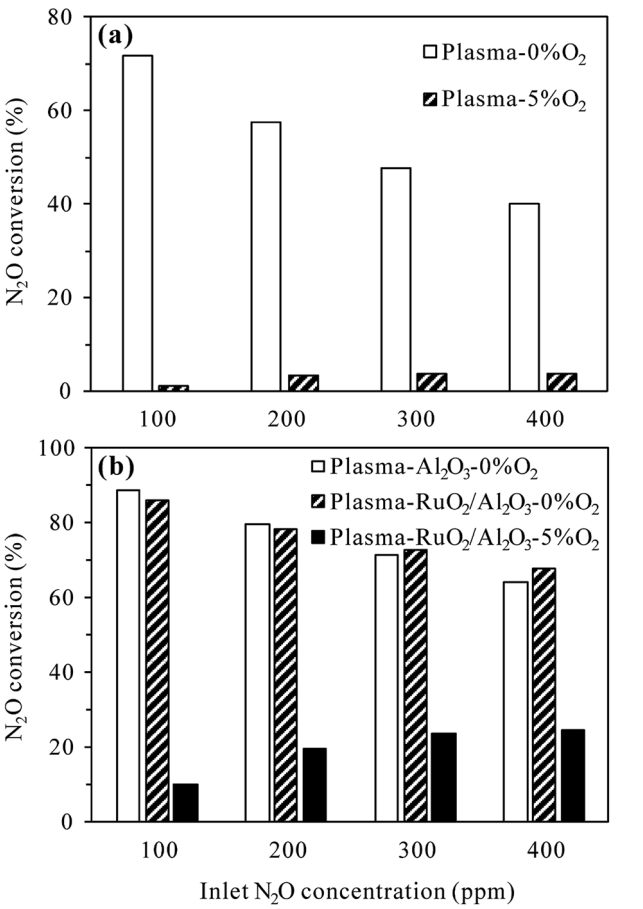

Fig. 8 Effects of inlet N_2O concentration on N_2O conversion in (a) plasma and (b) plasma-catalytic reactors at 300 °C (O_2 content: 0% or 5%; discharge power: 22 W for the plasma process and 34 W for the plasma-catalytic process).

(reaction (R2)), reducing the amount of $N_2(A^3\Sigma_u^+)$ species for N_2O formation (reaction (R3)).

For the plasma-catalytic process (Fig. 8(b)), at a given discharge power of 34 W, the conversion of N_2O without O_2 also decreased with increasing inlet N_2O concentration, but the decrease was less significant compared to that in the plasma process, proving the higher capacity of plasma-catalytic process in decomposing N_2O. Besides, it was noticed that the difference in the N_2O conversion between the plasma-Al_2O_3 and plasma-RuO_2/Al_2O_3 processes was insignificant in the absence of O_2, indicating the minor role of RuO_2 in promoting N_2O decomposition under N_2 atmosphere although RuO_2 greatly improved the N_2O conversion under N_2–O_2 atmosphere (Fig. 5 and 7).

As in the plasma process (Fig. 8(a)), the conversion of N_2O in the plasma-RuO_2/Al_2O_3 process also increased with the increase of inlet N_2O concentration in the presence of 5% O_2, especially from 100 to 200 and 300 ppm (Fig. 8(b)). Further increasing the inlet N_2O concentration, *e.g.*, to 400 ppm, showed limited effects in enhancing the N_2O conversion, probably due to the limited amount of reactive species ($N_2(A^3\Sigma_u^+)$ and $O(^1D)$) produced under a given discharge power for N_2O conversion. From the point of fully utilizing the generated reactive species and reducing the negative influence of O_2 on N_2O conversion, dilute N_2O in N_2–O_2 mixture should be concentrated, *e.g.*, by adsorption–desorption process before being converted by the plasma-catalytic process.[20]

In addition, it is noteworthy that for the same inlet N_2O concentration of 100 ppm and background gas of N_2, N_2O conversion in the plasma process increased from 47.1% at room temperature (Fig. 3) to 71.6% at 300 °C (Fig. 8(a)) for the same discharge power of 22 W. Similarly, N_2O conversion in the plasma-Al_2O_3 process increased from 66.2% at room temperature (Fig. 3) to 88.7% at 300 °C (Fig. 8(b)) for the same discharge power of 34 W. These results suggest that N_2O in N_2 could be decomposed more efficiently by plasma and plasma-catalytic processes at higher reaction temperature.

3.3 Mechanism of N_2O conversion

3.3.1 N_2O conversion pathways. On-line FT-IR (Fig. S3†) and NO_x measurement results show that under N_2 atmosphere, no other nitrogen oxide species were produced during the plasma and plasma-catalytic decomposition of N_2O regardless of the reaction temperature. O radicals generated in (R2) should have recombined and/or reacted with N_2O ((R6)) to give out O_2 as the final product instead of being consumed for NO/NO_2 production. In other words, N_2O was degraded to N_2 and O_2 by discharge in N_2 in both the presence and absence of catalyst and at both room and high temperature. Trinh *et al.*[20] proposed similar mechanism for direct decomposition of N_2O in N_2 DBD plasma.

On the other hand, as stated in Section 3.2, N_2O in N_2–O_2 mixture could be removed by plasma and plasma-catalytic processes only at high temperature. Fig. S4† shows typical FT-IR spectra of the effluents of plasma and plasma-catalytic reactors with and without 400 ppm-N_2O in the inlet gas (O_2 content 5%) and before and after discharge at 300 °C. Clearly,

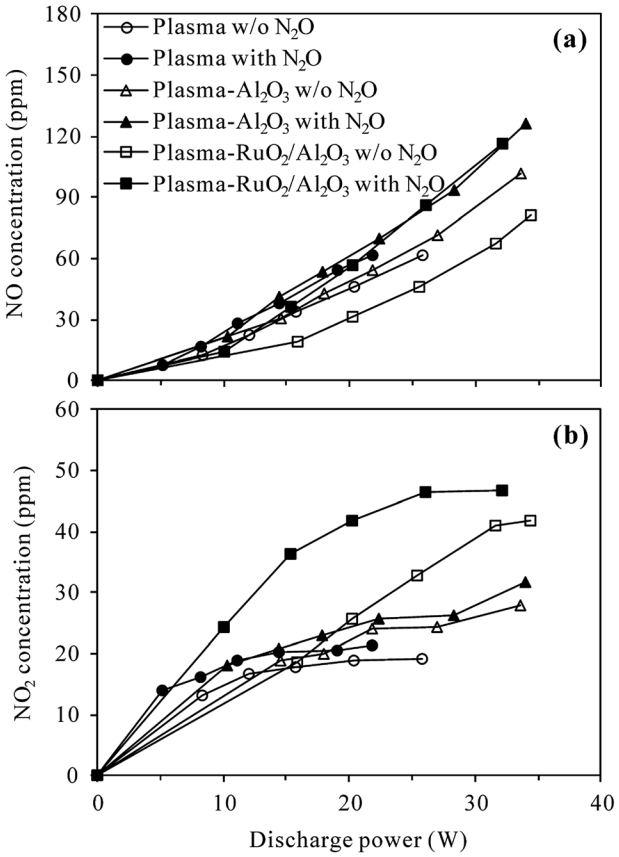

Fig. 9 Concentrations of (a) NO and (b) NO_2 formed with and without 400 ppm N_2O in the inlet gas of plasma and plasma-catalytic reactors at 300 °C (O_2 content: 5%).

discharge in N_2–O_2 mixture at 300 °C produced N_2O, NO and NO_2 as byproducts no matter the catalyst was present or not. When N_2O was introduced into the N_2–O_2 mixture, NO and NO_2 were also detected besides the residual N_2O. In order to clarify whether N_2O was converted to NO and NO_2 under N_2–O_2 atmosphere, the outlet concentrations of NO and NO_2 detected with and without 400 ppm-N_2O in the inlet gas were compared in Fig. 9.

Overall, NO and NO_2 concentrations increased with the increase of discharge power and the presence of 400 ppm-N_2O in the N_2–O_2 mixture did not obviously change the variation trends of NO or NO_2 concentrations. For a given discharge power, however, higher concentrations of NO and NO_2 were always detected when N_2O was introduced, especially in the plasma-RuO_2/Al_2O_3 process. This result revealed that N_2O was partially transformed into NO and NO_2 during the O_2-containing conversion processes, being in agreement with the observations of Krawczyk *et al.*[24,25] Table 1 lists the selectivity of NO, NO_2 and NO_x (NO + NO_2) at typical discharge power in the plasma and plasma-catalytic processes. As seen, the selectivity of NO_x ranged from 28.7% of the plasma-Al_2O_3 process at 34.0 W to 79.5% of the plasma process at 14.4 W. Other removed N_2O should have been degraded to benign N_2 and O_2 since no N-containing byproducts other than NO and NO_2 were observed.

Table 1 Selectivity of NO, NO_2 and NO_x (NO + NO_2) at typical discharge power in plasma and plasma-catalytic processes (inlet N_2O: 400 ppm; O_2 content: 5%; reaction temperature: 300 °C)

Process	Discharge power (W)	Selectivity of NO (%)	Selectivity of NO_2 (%)	Selectivity of NO_x (%)
Plasma	14.4	59.2	20.3	79.5
	21.8	37.1	7.6	44.7
Plasma-Al_2O_3	14.4	34.0	6.5	40.5
	34.0	24.7	4.0	28.7
Plasma-RuO_2/Al_2O_3	15.4	36.9	38.7	75.6
	32.1	28.4	3.4	31.8

Table 1 also shows that compared to the plasma process, the selectivity of NO_x was relatively low in the plasma-catalytic process, indicating that catalyst packed in the discharge zone promoted N_2O decomposition to N_2 and O_2 to a larger extent than oxidation to NO and NO_2. For all processes, the selectivity of NO and NO_2 decreased with the increase of discharge power, probably due to the substantial increase of NO and NO_2 formation from plasma-induced reactions between N_2 and O_2 which competitively consumed oxidative species, as shown in reactions (R9)–(R12).[27,29,32,37] Besides, the selectivity of NO was much higher than that of NO_2 except at low discharge power of the plasma-RuO_2/Al_2O_3 process. This can be easily ascribed to the step-wise oxidation of N_2O (first (R5) and then (R11) and (R12)) under oxidative plasma atmosphere.[27,32,37]

$$N_2(A^3\Sigma_u^+) + O \rightarrow NO + N(^2D) \quad (R9)$$

$$N(^2D) + O_2 \rightarrow NO + O \quad (R10)$$

$$NO + O + M \rightarrow NO_2 + M \quad (M = N_2, O_2, NO, NO_2, N_2O) \quad (R11)$$

$$NO + O_3 \rightarrow NO_2 + O_2 \quad (R12)$$

Compared to Al_2O_3 catalyst, RuO_2/Al_2O_3 catalyst significantly enhanced the selectivity of NO_2 at low discharge power. At higher discharge power, however, the difference in the selectivity of NO and NO_2 between the two plasma-catalytic processes became insignificant. At the relatively high discharge power tested, more than 40% and *ca.* 30% of the removed nitrogen in N_2O was transformed into NO_x in the plasma and plasma-catalytic process, respectively.

3.3.2 Synergy mechanism of plasma and catalyst for N_2O conversion under N_2–O_2 atmosphere. From the above-mentioned analysis, it can be concluded that introducing catalyst, especially RuO_2/Al_2O_3 into the discharge zone significantly enhanced the conversion of N_2O and promoted N_2O decomposition to N_2 and O_2 under N_2–O_2 atmosphere. Fig. 10 shows the XRD patterns of Al_2O_3 and RuO_2/Al_2O_3 catalysts before and after use in plasma-catalytic conversion of N_2O at 300 °C. From the XRD analysis, cubic Al_2O_3 was observed for all catalyst samples and tetragonal RuO_2 was formed over the RuO_2/Al_2O_3 catalyst. For both Al_2O_3 and RuO_2/Al_2O_3 catalysts, the XRD patterns were almost unchanged after use, indicating

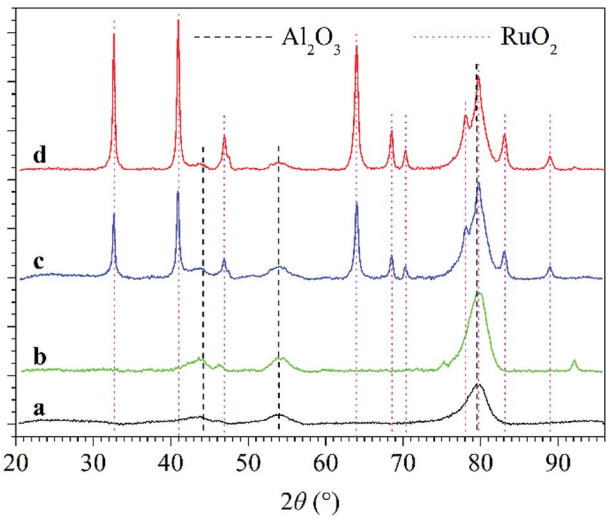

Fig. 10 XRD patterns of Al_2O_3 and RuO_2/Al_2O_3 catalysts: (line a) fresh Al_2O_3 catalyst; (line b) Al_2O_3 catalyst after use in plasma-catalytic conversion of N_2O at 300 °C; (line c) fresh RuO_2/Al_2O_3 catalyst; (line d) RuO_2/Al_2O_3 catalyst after use in plasma-catalytic conversion of N_2O at 300 °C.

that neither plasma nor the N_2O conversion reactions changed the phase composition of the catalysts.

According to literatures, the decomposition of N_2O over metal oxide catalysts can be expressed as a Langmuir–Hinshelwood mechanism:

$$N_2O + * \rightarrow N_2 + O^* \quad (R13)$$

$$O^* + O^* \rightarrow O_2 + 2^* \quad (R14)$$

where * stands for an active site of the catalyst.[3,23] In this mechanism, the adsorbed surface oxygen (O*) migrates from one active site to another to form O_2 by recombination, which is known to be the rate-determining step.[3,23] Applying DBD plasma in the RuO_2/Al_2O_3 catalyst bed could not only initiate gas-phase conversion of N_2O ((R2), (R5) and (R6)), but also accelerate the catalytic conversion of N_2O by speeding up the consumption of adsorbed surface oxygen (O*), *e.g.*, *via* reaction (R15) to regenerate the active sites.[23] In fact, the scavenging of O* by O radicals (reaction (R15)) also explained the decreased selectivity of NO_x

(increased selectivity of N_2 and O_2) in the presence of catalyst (Table 1), revealing the synergy of plasma and catalyst in promoting N_2O decomposition.

$$O + O^* \rightarrow O_2 + * \quad \text{(R15)}$$

4. Conclusions

In the present work, conversion of dilute N_2O in N_2 and N_2–O_2 mixtures by plasma and plasma-catalytic processes was investigated at both room and high temperature (300 °C). It is found that N_2O in N_2 can be effectively decomposed to N_2 and O_2 by plasma and plasma-catalytic processes at both room and high temperature, with much higher decomposition efficiency at 300 °C than at room temperature for the same discharge power. However, N_2O in N_2–O_2 mixture can be removed only at high temperature, producing not only N_2 and O_2 but also NO and NO_2. Production and conversion of N_2O occur simultaneously during the plasma and plasma-catalytic processing of N_2O in N_2–O_2 mixture, with production and conversion being the dominant process at room and high temperature, respectively.

N_2O conversion increases with the increase of discharge power and decreases with the increase of O_2 content. The negative influence of O_2 on N_2O conversion could be suppressed to some extent by concentrating N_2O in N_2–O_2 mixture which increases the involvement of plasma reactive species (*e.g.*, $N_2(A^3\Sigma_u^+)$ and $O(^1D)$) in N_2O conversion. Introducing catalyst, especially RuO_2/Al_2O_3 into the discharge zone significantly enhances the conversion of N_2O and improves the selectivity of N_2O decomposition under N_2–O_2 atmosphere, revealing the synergy of plasma and catalyst in promoting N_2O conversion, especially its decomposition to N_2 and O_2. The combined plasma-catalytic processing may be an efficient way for reducing N_2O emissions from combustion and industrial sources.

Conflicts of interest

There are no conflicts to declare.

Acknowledgements

This work was supported by the National Natural Science Foundation of China (grant numbers 21707004, 51638001) and the Natural Science Foundation of Beijing Municipality (grant number 8152011).

References

1 J. Pérez-RamíRez, F. Kapteijn, K. Schöffel and J. A. Moulijn, *Appl. Catal., B*, 2003, **44**, 117–151.
2 K. R. Sistani, M. Jn-Baptiste, N. Lovanh and K. L. Cook, *J. Environ. Qual.*, 2011, **40**, 1797–1805.
3 M. Konsolakis, *ACS Catal.*, 2015, **5**, 6397–6421.
4 A. Ates, A. Reitzmann, C. Hardacre and H. Yalcin, *Appl. Catal., A*, 2011, **407**, 67–75.
5 F. Zhang, X. Wang, X. Zhang, M. Turxun, H. Yu and J. Zhao, *Chem. Eng. J.*, 2014, **256**, 365–371.
6 M. Konsolakis, F. Aligizou, G. Goula and I. V. Yentekakis, *Chem. Eng. J.*, 2013, **230**, 286–295.
7 S. S. Kim, S. J. Lee and S. C. Hong, *Chem. Eng. J.*, 2011, **169**, 173–179.
8 Z. Liu, C. He, B. Chen and H. Liu, *Catal. Today*, 2017, **297**, 78–83.
9 H. L. Chen, H. M. Lee, S. H. Chen, M. B. Chang, S. J. Yu and S. N. Li, *Environ. Sci. Technol.*, 2009, **43**, 2216–2227.
10 J. V. Durme, J. Dewulf, C. Leys and H. V. Langenhove, *Appl. Catal., B*, 2008, **78**, 324–333.
11 X. Fan, T. L. Zhu, Y. F. Sun and X. Yan, *J. Hazard. Mater.*, 2011, **196**, 380–385.
12 Y. J. Wan, X. Fan and T. L. Zhu, *Chem. Eng. J.*, 2011, **171**, 314–319.
13 X. Fan, T. L. Zhu, Y. J. Wan and X. Yan, *J. Hazard. Mater.*, 2010, **180**, 616–621.
14 X. Fan, T. L. Zhu, M. Y. Wang and X. M. Li, *Chemosphere*, 2009, **75**, 1301–1306.
15 Q. Yu, Y. Gao, X. Tang, H. Yi, R. Zhang, S. Zhao, F. Gao and Y. Zhou, *Catal. Commun.*, 2018, **110**, 18–22.
16 A. Mizuno, *Catal. Today*, 2013, **211**, 2–8.
17 X. Hu, J. Nicholas, J. Zhang, T. M. Linjewile, P. D. Filippis and P. K. Agarwal, *Fuel*, 2002, **81**, 1259–1268.
18 G. B. Zhao, X. D. Hu, M. D. Argyle and M. Radosz, *Ind. Eng. Chem. Res.*, 2004, **43**, 5077–5088.
19 S. Mahammadunnisa, E. L. Reddy, P. R. M. K. Reddy and C. Subrahmanyam, *Plasma Processes Polym.*, 2013, **10**, 444–450.
20 Q. Trinh, S. H. Kim and Y. S. Mok, *Chem. Eng. J.*, 2016, **302**, 12–22.
21 D. H. Lee and T. Kim, N_2O decomposition by catalyst-assisted cold plasma, *20th Int. Symp. Plasma Chem.*, Philadelphia, USA, 2012.
22 H. Hu, H. Huang, J. Xu, Q. Yang and G. Tao, *Plasma Sci. Technol.*, 2015, **17**, 1043–1047.
23 J. Jo, Q. H. Trinh, S. H. Kim and Y. S. Mok, *Catal. Today*, 2018, **310**, 42–48.
24 K. Krawczyk and M. Młotek, *Appl. Catal., B*, 2001, **30**, 233–245.
25 K. Schmidt-Szałowski, K. Krawczyk and M. Młotek, *J. Adv. Oxid. Technol.*, 2007, **10**, 330–336.
26 G. Pekridis, C. Athanasiou, M. Konsolakis, I. V. Yentekakis and G. E. Marnellos, *Top. Catal.*, 2009, **52**, 1880–1887.
27 I. A. Kossyi, A. Y. Kostinsky, A. A. Matveyev and V. P. Silakov, *Plasma Sources Sci. Technol.*, 1992, **1**, 207–220.
28 M. P. Iannuzzi, J. B. Jeffries and F. Kaufman, *Chem. Phys. Lett.*, 1982, **87**, 570–574.
29 X. Tang, J. Wang, H. Yi, S. Zhao, F. Gao, Y. Huang, R. Zhang and Z. Yang, *Energy Fuels*, 2017, **31**, 13901–13908.
30 J. T. Herron and D. S. Green, *Plasma Chem. Plasma Process.*, 2001, **21**, 459–481.
31 K. Krawczyk, *IEEE Trans. Plasma Sci.*, 2009, **37**, 884–889.
32 G. B. Zhao, S. Garikipati, X. D. Hu, M. D. Argyle and M. Radosz, *AIChE J.*, 2005, **51**, 1800–1812.

33 G. Sathiamoorthy, S. Kalyana, W. C. Finney, R. J. Clark and B. R. Locke, *Ind. Eng. Chem. Res.*, 1999, **38**, 1844–1855.
34 S. Kanazawa, J. S. Chang, G. F. Round, G. Sheng, T. Ohkubo, Y. Nomoto and T. Adachi, *J. Electrost.*, 1997, **40–41**, 651–656.
35 Y. S. Mok, J. H. Kim, I. S. Nam and S. W. Ham, *Ind. Eng. Chem. Res.*, 2000, **39**, 3938–3944.
36 M. S. Bak, W. Kim and M. A. Cappelli, *Appl. Phys. Lett.*, 2011, **98**, 011502.
37 Y. Zhang, X. Tang, H. Yi, Q. Yu, J. Wang, F. Gao, Y. Gao, D. Li and Y. Cao, *RSC Adv.*, 2016, **6**, 63946–63953.